mediated hematopoiesis from human embryonic stem cells. Exp Hematol 2004;32:1000-1009.
33. Wang X, Hisha H, Taketani S, et al. Neural cell adhesion molecule contributes to hemopoiesis-supporting capacity of stromal cell lines. Stem Cells 2005;23:1389-1399.
34. Zwaka TP, Thomson JA. Homologous recombination in human embryonic stem cells. Nat Biotechnol 2003;21:319-321.
35. Urbach A, Schuldiner M, Benvenisty N. Modeling for Lesch-Nyhan disease by gene targeting in human embryonic stem cells. Stem Cells 2004;22:635-641.
36. Matsumura H, Tada M, Otsuji T, et al. Targeted chromosome elimination from ES-somatic hybrid cells. Nat Methods 2007;4:23-25.

Figure 1. Culture protocol and morphological changes of human ES cell-derived cells during differentiation culture. (A) The schedule for the culture to induce differentiation of human ES cells into ES-DC is schematically depicted. (B) Undifferentiated human ES cells on PEF feeder layer. (C-E) ES cell-derived cells on day 3 (C), day 11 (D), and day 15 (E) in the 1st step. (F) Cells on day 6 in the 2nd step. (G-J) Cells on day 1 (G), day 3 (H), and day 6 (I, J) in the 3rd step. Cells shown in (I, J) had been stimulated with TNF-α plus LPS for 2 days.

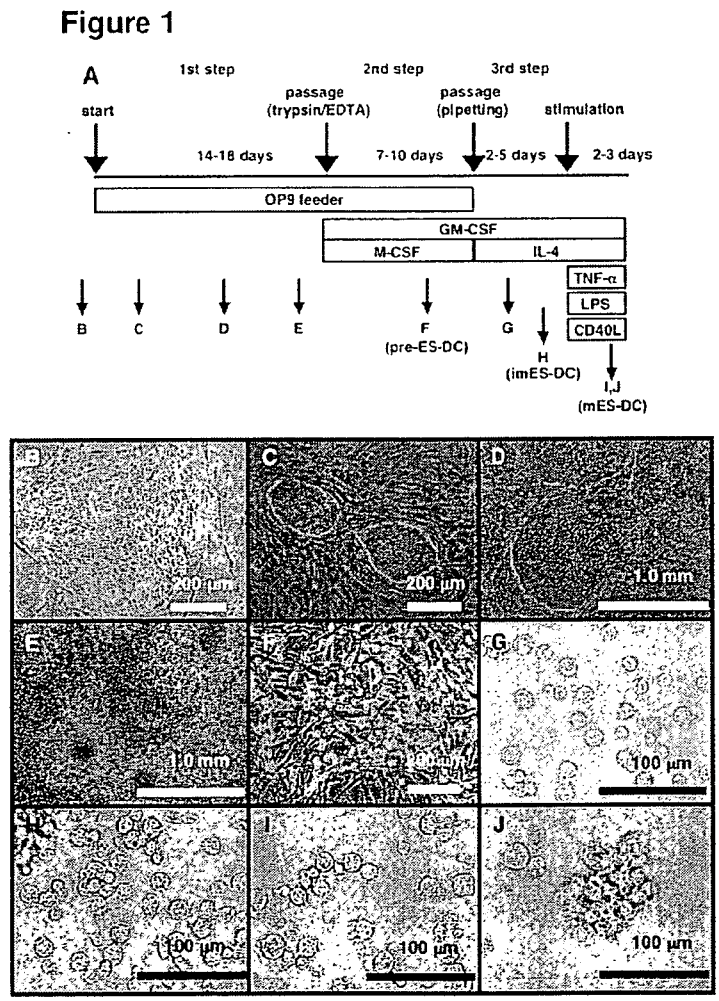

Figure 2. Cell surface phenotypes of human ES-DC. (A) ES cell-derived floating cells harvested on day 6 in the 2nd step were analyzed on the cell surface expression of CD34, CD45, CD31, CD43, CD11b, and CD14. (B) ES cell-derived cells harvested on day 8 in the 2nd step (pre-ES-DC), or from the 3 rd step before (immature ES-DC: imES-DC) or after (mature ES-DC: mES-DC) addition of maturation stimuli were analyzed on the cell surface expression of CD80, CD83, CD86, CD40, HLA-DR, and HLA class I. Staining profiles with specific Ab (thick lines) and isotype-matched control Ab (thin broken lines) are shown.

Figure 2

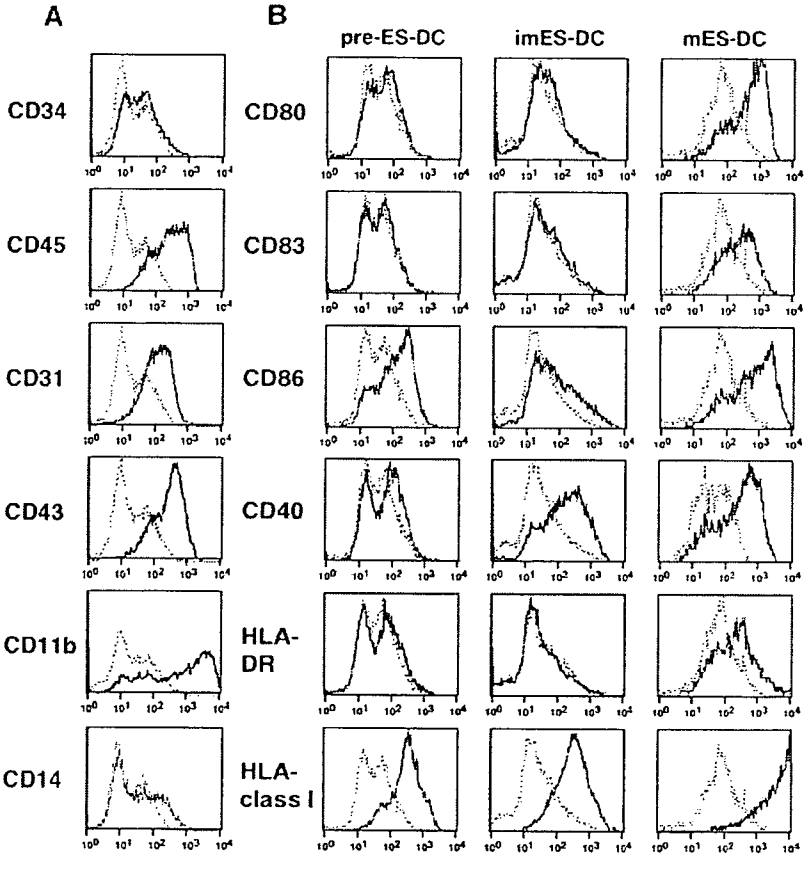

Figure 3. Production of TNF-α and IL-12 by ES-DC. ES-DC were recovered from the culture (3rd step day 4) and re-plated (1.2 x 10^5 cells / 150 μl / in 96-well culture plates) in the presence or absence of soluble CD40-ligand (20 ng/ ml), LPS (3 μg /ml), or OK432 (10 μg /ml) as indicated. After 60 hours, supernatant was collected and concentration of TNF-α and IL-12 p70 was measured by ELISA. Data are indicated by mean value + standard deviation of duplicate cultures.

Figure 3

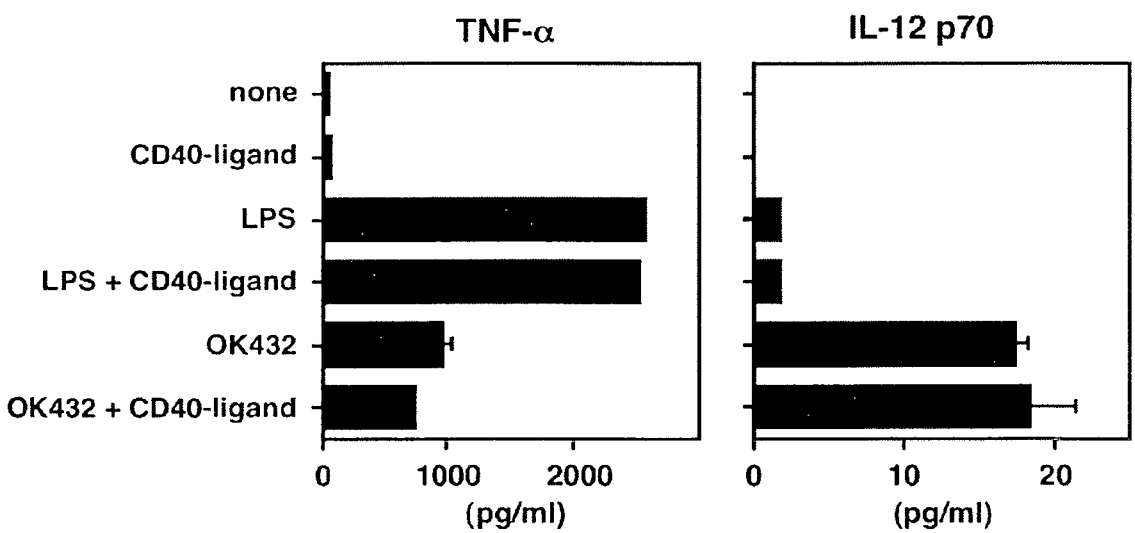

Figure 4. Stimulation of allogeneic T cells and antigen presentation by human ES-DC. (A) The indicated numbers of mature ES-DC (circles), immature ES-DC (diamonds), or pre-ES-DC (squares) were X-ray-irradiated (40 Gy) and co-cultured with allogeneic human peripheral blood T cells (4 x10^4/ well) in a 96-well round-bottomed culture plate for 5 days. Proliferation of T cells in the last 16 hours of the culture was measured based on [^{3}H]-thymidine uptake. The data are indicated as the mean value +/- standard deviation of duplicate cultures. (B) Indicated numbers of KhES-1-derived mature ES-DC pre-pulsed with $GAD65_{111-131}$ peptide (squares) or those left un-pulsed (diamonds) were co-cultured with a GAD65-specific, HLA-DR53-restricted human $CD4^+$ T cell clone, SA32.5 (3 x10^4 T cells / well) for 3 days. Proliferation of the T cells in the last 16 hours of the culture was measured by [^{3}H]-thymidine uptake. (C) Mature KhES-1-derived ES-DC (1 x 10^4 / well) were co-cultured with SA32.5 T cells (3 x 10^4 / well) in the presence of indicated concentrations of GST-GAD65 recombinant protein (squares) or GST protein (diamonds) for 3 days. Proliferation of the T cells in the last 16 h of the culture was measured by [^{3}H]-thymidine uptake.

Figure 4

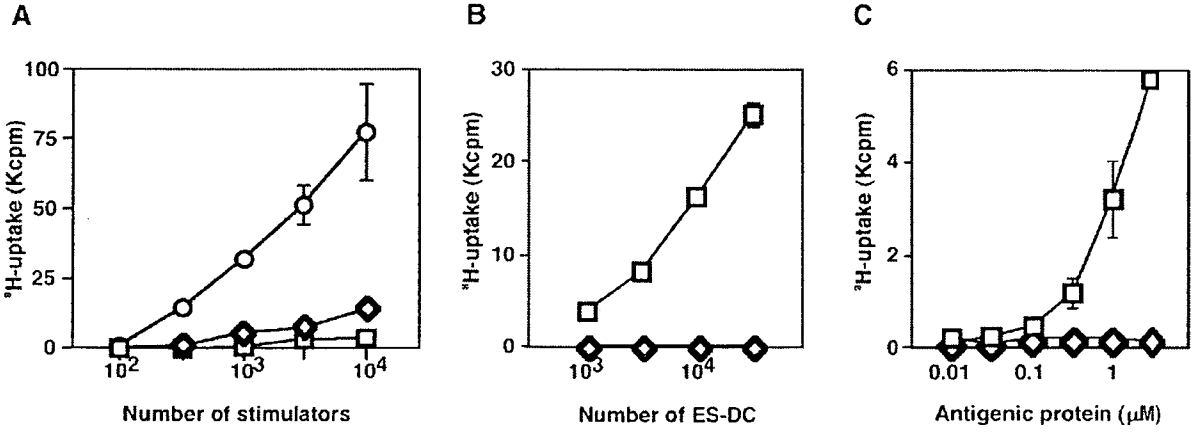

Figure 5. Genetic modification of human ES-DC. (A) The structure of the expression vector for human PD-L1. The expression of PD-L1 was driven by CAG promoter and the PD-L1-coding sequence was followed by IRES-neomycin-resistance gene (Neo-R), a selection marker. The open box in the CAG promoter indicates the exon 1 of the rabbit β-actin gene contained in CAG promoter. (B) Transgene-derived PD-L1 expressed in immature ES-DC originated from transfectant ES cells was detected by flowcytometric analysis (ES-DC-PDL1, clone 28). As a control, the staining profile of ES-DC derived from parental ES cell line (K1ES-DC) is shown. Specific staining with anti-human-PD-L1 monoclonal Ab (thick line) and isotype-matched control staining (thin broken line) are shown. (C) Alloreactive response of T cells (4×10^4 / well) co-cultured with immature ES-DC (1×10^4 / well) derived from the PD-L1-transfectant ES cells (ES-DC-PDL1, clone 28) or those derived from parental ES cell line (K1ES-DC) is shown. The culture was done under the same conditions as those shown in Figure 3A except that anti-PD-L1 blocking Ab or isotype-matched mouse IgG1 was added to the culture. The statistical significance of the differences between the T cell responses was indicated by asterisks (*, $P<0.05$: **, $P<0.01$). (D) The structure of expression vector for human invariant chain (Ii/CD74) including GAD65-derived epitope. The CLIP region of the Ii-coding sequence was replaced with an oligo DNA encoding $GAD65_{115\text{-}127}$. (E) Intracellular CD74 expressed in pre-ES-DC originated from transfectant ES cell clone (pre-ES-DC-hIi, clone 23) and parental ES cell line (pre-K1ES-DC) was detected by a flowcytometric analysis. Specific staining with anti-human-CD74 mAb (thick lines) and isotype-matched control staining (thin broken lines) are shown. The values in the figure indicate the difference of mean fluorescence intensity (delta MFI) between staining with the anti-CD74 and isotype-matched control Ab. (F) SA32.5 T cells (3×10^4 / well) were co-cultured with indicated numbers of mature ES-DC-hIi clone 23 (squares) or non-transfectant ES-DC (circles) in the absence of exogenous antigen for 3 days. The proliferation of the T cells in the last 16 h of the culture was measured by the [^{3}H]-thymidine uptake.

Figure 5

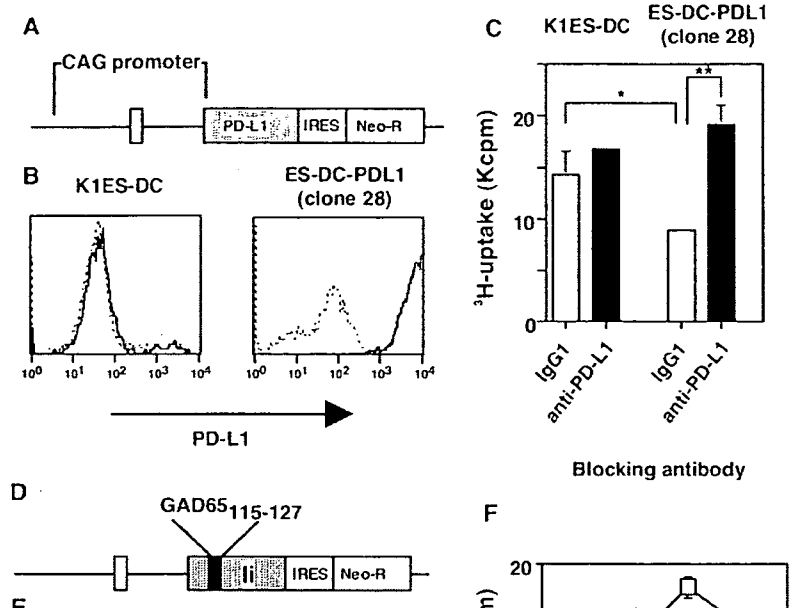

Figure 6. Generation of ES-DC from cynomolgus monkey ES cells. (A-C) The morphology of cynomolgus monkey ES cell-derived differentiating cells (pre-ES-DC) at day 7 in the 2nd step (A) and those in the 3rd step before (B) or after (C) the addition of maturation stimuli is shown. (D) Cynomolgus monkey ES cell-derived cells harvested on day 8 in the 2nd step (pre-ES-DC), or from the 3rd step before (immature ES-DC: im ES-DC) or after (mature ES-DC: m ES-DC) addition of maturation stimuli were analyzed on the cell surface expression of CD80, CD86, CD40, CyLA-DR, and CyLA class I. Staining patterns with specific monoclonal Ab (thick lines) and isotype-matched controls (thin broken lines) are shown. (E) Indicated numbers of mature ES-DC (squares), immature ES-DC (diamonds), pre-ES-DC (circles), or undifferentiated cynomologus ES cells (triangles) were X-ray-irradiated (40 Gy) and co-cultured with allogeneic cynomolgus monkey peripheral blood T cells (4 x 10^4/ well) in a 96-well round-bottomed culture plate for 5 days. The proliferative responses of T cells in the last 16 hours of the culture were measured based on the [^{3}H]-thymidine uptake.

Figure 6

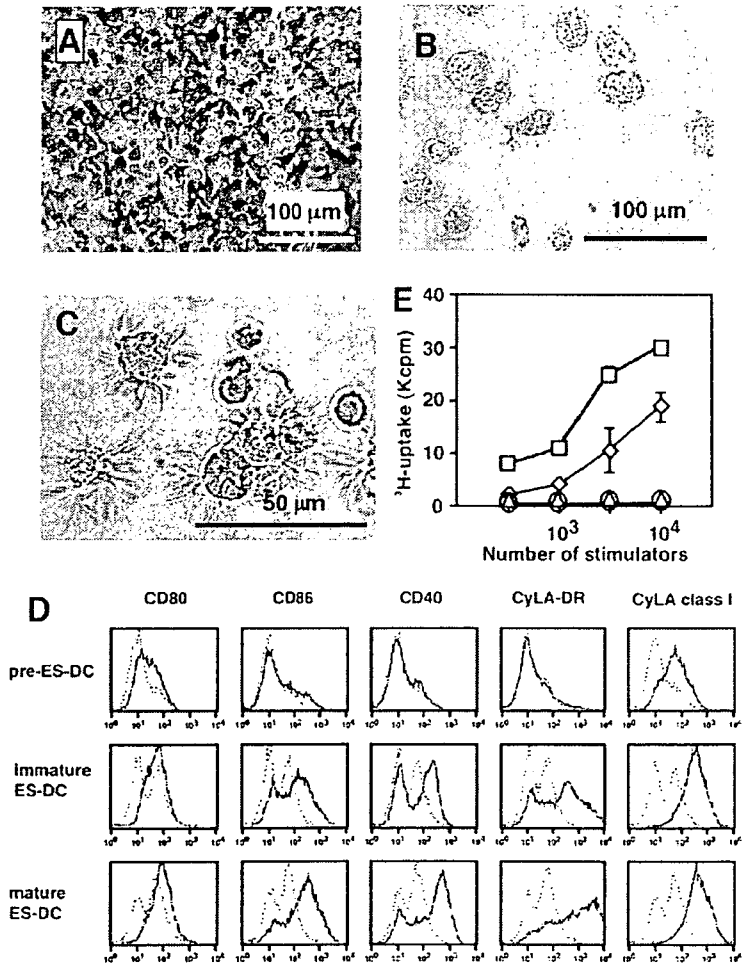

Figure 7. Antigen presentation to human T cells by genetically modified cynomolgus monkey ES-DC. (A) The structure of HLA-DRB4*0103 expression vector is shown. The open box indicates non-coding 1st exon of rabbit β-actin gene included in the CAG promoter. RT-PCR with PCR primers indicated by arrow-heads generated PCR products of 286 bp from the transgene-derived mRNA. (B) The results of an RT-PCR analysis of parental cynomolgus ES cells (cES) and a transfectant ES cell clone (cES-DRB4) and derivative ES-DC on the expression of transgene-derived mRNA (CAG-DRB4). The PCR products for HPRT transcript amplified from the same cDNA samples are also shown as control. (C) Indicated numbers of DRB4-transfectant ES-DC (squares) or non-transfectant ES-DC (circles) were pre-loaded with $GAD65_{111-131}$ peptide, X-ray-irradiated (40 Gy), and co-cultured with SA32.5 T cells (3 x 10^4 / well) for 3 days. The proliferation of the T cells in the last 16 h of the culture was measured by the [^{3}H]-thymidine uptake. (D) DRB4-transfectnat ES-DC (diamonds) (1 x 10^4 / well) or non-transfectant ES-DC (squares) were co-cultured with SA32.5 T cells (3 x 10^4 / well) in the presence of the indicated concentration of GST-GAD recombinant protein for 3 days. DRB4-transfectnat ES-DC and SA32.5 T cells were co-cultured also in the presence of GST protein (circles). The proliferation of the T cells in the last 16 hours of the culture was measured by the [^{3}H]-thymidine uptake.

Figure 7

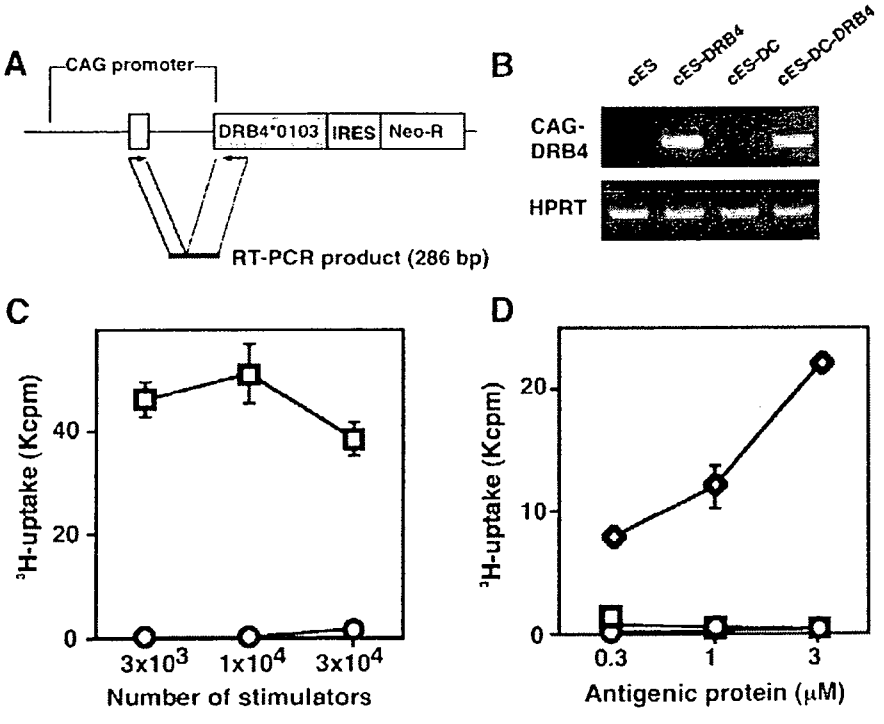

Genetically Manipulated Human Embryonic Stem Cell-derived Dendritic Cells with Immune Regulatory Function

Satoru Senju, Hirofumi Suemori, Hitoshi Zembutsu, Yasushi Uemura, Shinya Hirata, Daiki Fukuma, Hidetake Matsuyoshi, Manami Shimomura, Miwa Haruta, Satoshi Fukushima, Yusuke Matsunaga, Toyomasa Katagiri, Yusuke Nakamura, Masataka Furuya, Norio Nakatsuji and Yasuharu Nishimura

Stem Cells published online Aug 9, 2007;
DOI: 10.1634/stemcells.2007-0321

Disease-associated mutations in *CIAS1* induce cathepsin B–dependent rapid cell death of human THP-1 monocytic cells

Akihiro Fujisawa,[1] Naotomo Kambe,[1] Megumu Saito,[2] Ryuta Nishikomori,[2] Hideaki Tanizaki,[1] Nobuo Kanazawa,[1,3] Souichi Adachi,[2] Toshio Heike,[2] Junji Sagara,[4] Takashi Suda,[5] Tatsutoshi Nakahata,[2] and Yoshiki Miyachi[1]

[1]Department of Dermatology, Kyoto University Graduate School of Medicine, Japan; [2]Department of Pediatrics, Kyoto University Graduate School of Medicine, Japan; [3]Department of Dermatology, Wakayama Medical University, Japan; [4]Department of Biochemical Laboratory Science, School of Health Science, Shinshu University, Nagano, Japan; [5]Division of Immunology and Molecular Biology, Cancer Research Institute, Kanazawa University, Ishikawa, Japan

Mutations in the cold-induced autoinflammatory syndrome 1 (*CIAS1*) gene are associated with a spectrum of autoinflammatory diseases, including familial cold autoinflammatory syndrome, Muckle-Wells syndrome, and chronic infantile neurologic, cutaneous, articular syndrome, also known as neonatal-onset multisystem inflammatory disease. *CIAS1* encodes cryopyrin, a protein that localizes to the cytosol and functions as pattern recognition receptor. Cryopyrin also participates in nuclear factor-κB regulation and caspase-1–mediated maturation of interleukin 1β. In this study, we showed that disease-associated mutations in *CIAS1* induced rapid cell death of THP-1 monocytic cells. The features of cell death, including 7-AAD staining, the presence of cellular edema, and early membrane damage resulting in lactate dehydrogenase (LDH) release, indicated that it was more likely to be necrosis than apoptosis, and was effectively blocked with the cathepsin B–specific inhibitor CA-074-Me. CA-074-Me also suppressed induced by disease-associated mutation lysosomal leakage and mitochondrial damage. In addition, R837, a recently identified activator of cryopyrin-associated inflammasomes, induced cell death in wild type *CIAS1*-transfected THP-1 cells. These results indicated that monocytes undergo rapid cell death in a cathepsin B–dependent manner upon activation of cryopyrin, which is also a specific phenomenon induced by disease-associated mutation of *CIAS1*. (Blood. 2007;109:2903-2911)

Introduction

Chronic infantile neurologic, cutaneous, articular syndrome (CINCA; MIM #697115; Mendelian Inheritance in Man [MIM]; http://www.ncbi.nlm.nih.gov/entrez/query.fcgi?db=OMIM), also known as neonatal-onset multisystem inflammatory disease, is characterized by recurrent fever, an urticarial rash beginning in the neonatal period, arthropathy characterized by epiphyseal patellar overgrowth, growth retardation, chronic meningitis, papilledema, and hearing loss.[1,2] The gene responsible for the syndrome is known as cold-induced autoinflammatory syndrome 1 (*CIAS1*), and is associated with 2 less severe but phenotypically similar syndromes, familial cold autoinflammatory syndrome (FCAS; MIM #120100) and Muckle-Wells syndrome (MWS; MIM #191900).[3-7] *CIAS1*, also designated as *PYPAF1* and *NALP3*, is expressed in polymorphonuclear cells, monocytes, chondrocytes, and activated T cells.[6,8,9] Its product is cryopyrin, which contains an amino-terminal pyrin domain (PYD), a centrally located nucleotide-binding oligomerization domain (NOD), also called a NACHT domain, and several carboxy-terminal leucine-rich repeats (LRRs). Cryopyrin localizes to the cytosol and is believed to function as a pattern-recognition receptor.

Animals and plants have several types of so-called pattern-recognition receptors that distinguish characteristic molecular structures of microorganisms and activate innate immune responses. In mammals, Toll-like receptors (TLRs) are a well-characterized type of pattern-recognition receptor that recognize pathogen-associated molecular patterns via their extracellular LRRs.[10] Cryopyrin belongs to another class of mammalian pattern-recognition receptors that are homologous to plant disease resistance–associated NOD-LRR proteins (NLRs).[11,12] More than 20 genes encoding NLRs have been identified in the human genome, many of which contain a caspase-activating recruitment domain (CARD), or a PYD, in their amino-terminal region. Among the human NLRs, NOD1/CARD4 and NOD2/CARD15 were found to recognize the structure of a distinct bacterial peptidoglycan, namely γ-D-glutamyl-*meso*-diaminopimelic acid and muramyl dipeptide (MDP), respectively, via their intracellular LRRs. Recognition results in activation of nuclear factor κB (NF-κB) and caspase-9.[13-15] Several other members of the NLR family induce caspase-1–mediated maturation of interleukin (IL)-1β,[16-20] suggesting that these molecules also function as cytoplasmic receptors for the immune response. In addition to participating in NF-κB regulation,[21,22] cryopyrin activates caspase-1, and is involved in the conversion of the proform of IL-1β into the mature and biologically active molecule, along with an adaptor protein called apoptosis-associated speck-like protein containing a CARD (ASC), which also contains a PYD.[21,23] ASC was originally identified as a protein that generates speck-like aggregations in apoptotic HL-60 cells treated with chemotherapeutic agents.[24] Thus, ASC has been implicated in apoptosis,[25] but its role in disease-associated CIAS1 function and cell death has not been preciously described.

Submitted July 5, 2006; accepted November 22, 2006. Prepublished online as *Blood* First Edition Paper, December 12, 2006; DOI 10.1182/blood-2006-07-033597.

The online version of this manuscript contains a data supplement.

The publication costs of this article were defrayed in part by page charge payment. Therefore, and solely to indicate this fact, this article is hereby marked "advertisement" in accordance with 18 USC section 1734.

Programmed cell death is essential for proper development and maintenance of multicellular organisms. Caspases, a family of cysteine-aspatatic acid proteases that reside in an inactive zymogen form in the cytosol of virtually every cell, have long been considered the essential killer enzymes in all programmed cell death. However, in addition to caspases, increasing evidence suggests a role for lysosomal proteases in cell death, and in the clearance of infected cells.[26,27] Lysosomes contain a number of proteases, among them the cysteine protease cathepsin B and the aspartic protease cathepsin D, which are the most abundant and have most often been linked to cell death.[28-33]

Recently, we found that monocytes in patients with CINCA underwent rapid necrosis-like cell death after the induction of the *CIAS1* gene with lipopolysaccharide (M.S., R.N., N.K., A.F., H.T., T.H., Y.M., and T.N., manuscript submitted). In this study, we explored the mechanism, and found that disease-associated mutations of *CIAS1* provoked rapid cell death of THP-1 monocytes. Cell death did not exhibit the typical features of apoptosis, but appeared to be more like necrosis. Interestingly, several features of cell death induced by disease-associated *CIAS1* mutation were effectively blocked with the cathepsin B inhibitor CA-074-Me. In addition, a small synthetic antiviral molecule R837, recently identified as an activator of cryopyrin-associated inflammasome, induced cell death in wild-type *CIAS1*-transfected THP-1 cells. These results indicate that cryopyrin, when activated, participates in rapid necrosis-like cell death in a lysosomal cathepsin B–dependent manner.

Materials and methods

Reagents

The caspase inhibitors zVAD-fmk, zYVAD-cho, zIETD-fmk, and zLEHD-fmk were purchased from R&D Systems (Minneapolis, MN). The caspase-3 inhibitor zDEVD-fmk was obtained from Peptide Institute (Osaka, Japan), and the cathepsin B inhibitor CA-074-Me ([L-3-*trans*-(propylcarbamoyl) oxirane-2-carbonyl]-L-isoleucyl-L-proline methyl ester) was obtained from Calbiochem (Darmstadt, Germany). Nigericin and actinomycin D were purchased from Sigma-Aldrich (St Louis, MO). The small synthetic antiviral molecule imiquimod R837 was purchased from InvivoGen (San Diego, CA). Anti–caspase-1, anti–caspase-8, anti-Bid, and the apoptosis sampler kit containing rabbit-derived polyclonal antibodies (Abs) against caspase-3 and the corresponding cleaved form of caspase-3 were obtained from Cell Signaling Technology (Beverly, MA). Caspase-3 activity was measured using a Colorimetoric CaspACE Assay System (Promega, Madison, WI).

Plasmids

Expression plasmids for *CIAS1* and *ASC* in the pEF-BOS vector background have been previously described.[34] *CIAS1* was also cloned into the pIRES2-EGFP vector (Invitrogen, Carlsbad, CA). Mutants were generated using the QuikChange site-directed mutagenesis kit (Stratagene, La Jolla, CA), as described previously.[35] *NOD2/CARD15* and its disease-associated mutation, an asparagine-to-lysine substitution at amino acid (aa) 670 (N670K) in p3xFLAG-CMV, were previously described.[36] cDNAs encoding carboxy-terminal green fluorescent protein (GFP)–tagged *CIAS1* and its mutants were generated and subcloned into pcDNA5/TO (Invitrogen). The ability of each construct to induce NF-κB activation was assessed by a dual luciferase reporter assay in HEK293 human embryonic kidney cells, as previously described.[35]

Cell lines

Human monocytic THP-1 cells were maintained in RPMI-1640 medium (Sigma-Aldrich) supplemented with 10% fetal calf serum. Expression plasmids were introduced into THP-1 cells using cell line nucleofector kit V (Amaxa Biosystems, Cologne, Germany) according to the manufacturer's instructions with equipment program no. V-01. Treatment of the cells with 10 ng/mL phorbol 12-myristate 13-acetatae (PMA) dramatically improved gene expression and reduced spontaneous cell death induced by gene transfection without affecting cell death induced by the mutants of CIAS1 (data not shown). Therefore, we added PMA (10 ng/mL; Sigma-Aldrich) to the cells immediately following gene transfection. THP-1 cells were also incubated with 50 μM proteinase inhibitors where indicated. Because the expression of cryopyrin-GFP required more than 1 hour of incubation after transfection (Figure 1C), proteinase inhibitor was added to the culture

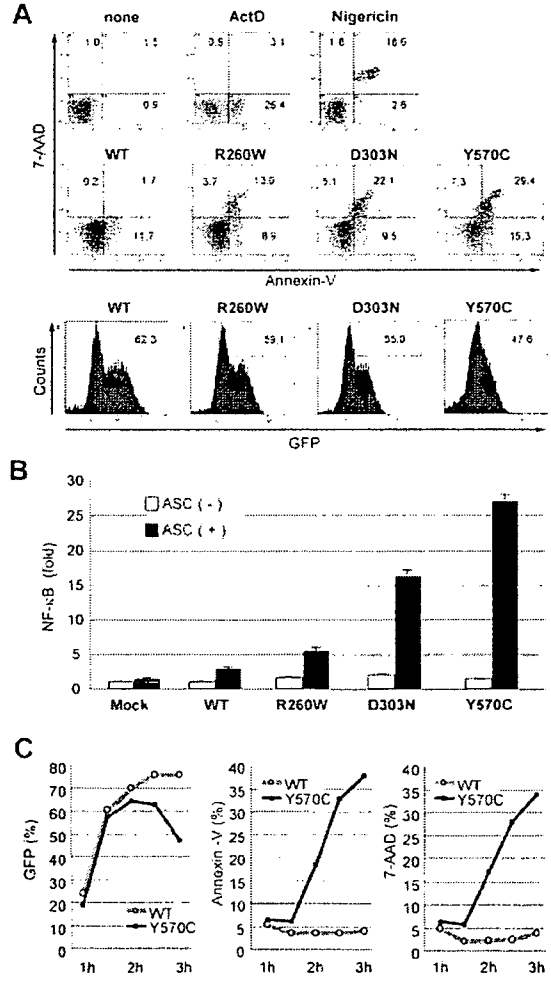

Figure 1. Autoinflammatory disease-associated mutations in *CIAS1* induce rapid cell death. (A) As the controls for cell death, 1 × 10^6 THP-1 cells were treated with 1 μg/mL actinomycin D (ActD) and 20 μM nigericin. 0.5 μg of plasmid encoding GFP-*CIAS1* or the disease-associated mutants (R260W, D303N, Y570C) were introduced into 1 × 10^6 THP-1 cells. After transfection (3 hours), cells were analyzed by flow cytometry, and the expression of *CIAS1* was monitored by measuring GFP fluorescence. Cell death was assessed as positive annexin V staining (apoptosis) or double positive for annexin V and 7-AAD (necrosis). The number in each quadrant shows the percentage of cells. (B) HEK293 cells were cotransfected with 20 ng of WT-*CIAS1* or the indicated mutants in the presence or absence of 20 ng of *ASC*. The ability to induce NF-κB activation was assessed by a dual luciferase reporter assay in HEK293 cells. Disease-associated mutants induced ASC-dependent NF-κB activation spontaneously. Values represent the mean of normalized data (mock without ASC = 1) of triplicate cultures, and error bars indicate SD. (C) Expression of GFP-*CIAS1* and annexin V and 7-AAD staining were monitored by flow cytometry. Expression of GFP was observed at 1 hour and 30 minutes after transfection, at which point annexin V/7-AAD–positive cells started to appear in the Y570C-transfected cell population. The percentage of Y570C-transfected cells that were annexin V/7-AAD positive increased in a time-dependent manner. Representative data from 3 independent analyses of similar results are shown.

medium just after gene transfection. The concentration of CA-074-Me (50 μM) used in this study was determined by monitoring the suppression of intracellular cathepsin B activity in THP-1 cells using a cathepsin B fluorogenic substate (Calbiochem; data not shown).

Flow cytometry

Transfection efficiency of GFP fusion protein constructs was assessed by flow cytometry (Epics XL-MCL; Beckman Coulter, Miami, FL). Cell death was analyzed using an annexin V–PE apoptosis detection kit (BD Pharmingen, San Diego, CA), and was classified as positive for annexin V (apoptosis), or double-positive for annexin V and 7-AAD (necrosis).

Assessment of lysosomal and mitochondrial integrity

For the evaluation of small scale of lysosomal leakage (ssΔLL) and loss of mitochondrial inner transmembrane potential ($\Delta\psi m$), cells were incubated with 1 μg/mL acridine orange (Invitrogen) and 1 μM MitoTracker DeepRed 633 (Invitrogen), respectively, in the culture medium for 15 minutes at 37°C, then washed in PBS. Cells were assessed by flow cytometry, and also observed with a confocal laser-scanning microscope (LSM510; Carl Zeiss, Jena, Germany) equipped with a 63×/1.2 water objective lens. LSM510 version 3.2 software was used to process images. For assessment of ssΔLL, we used CIAS1 and its variants without GFP tags, and evaluated nuclei by green fluorescence following acridine orange staining.

Measurement of IL-1β and LDH

For cytokine analysis, cells were cultured with or without lipopolysaccharide (LPS, 10 ng/mL; Sigma-Aldrich) and supernatants were collected. An enzyme-linked immunosorbent assay (ELISA) for IL-1β (eBioscience, San Diego, CA) was performed according to the manufacturer's protocol. Lactate dehydrogenase (LDH) that was spontaneously released from damaged cells into the culture supernatant was assessed using the CytoTox96 nonradioactive cytotoxicity assay kit from Promega.

Electron microscopy

Cells were fixed in 2% glutaraldehyde in phosphate buffer. Routine procedures for observation by electron microscopy were performed by SRL Inc (Tokyo, Japan).

Western blot analysis

Plasmid encoding wild-type (WT)-*CIAS1* or Y570C mutant (1 μg) was introduced into 2×10^6 THP-1 cells. After transfection (3 hours), cells were lysed in M-PER mammalian protein extraction reagent (Pierce, Rockford, IL) containing protease inhibitor cocktail. The concentration of protein in the cell lysates was measured using the Protein Assay Dye Reagent (BioRad, Hercules, CA). Denatured proteins in BioRad sample buffer were separated on a 12% polyacrylamide gel under reducing conditions with 5% 2-mercaptoethanol. After electrophoresis, proteins were transferred onto a membrane, and the membrane was incubated with primary Ab, followed by incubation with secondary Ab conjugated to horseradish peroxidase (Vector Laboratories, Burlingame, CA). Immunoreactive proteins were detected using an ECL Plus detection system (Amersham Biosciences, Piscataway, NJ).

Results

Disease-associated mutations in *CIAS1* induce rapid cell death in human THP-1 monocytic cells

Mutation of *CIAS1* is associated with FCAS, MWS, and CINCA, which represent a spectrum of diseases, and have been grouped together as cryopyrin-associated periodic syndrome (CAPS). Among these diseases, FCAS is the mildest, and CINCA is the most severe. In the current study, as the disease-associated mutations of *CIAS1*, we used the arginine-to-tryptophan substitution at aa 260 (R260W), which was identified in FCAS and MWS; the aspartic acid-to-asparagine substitution at aa 303 (D303N), which was identified in MWS and CINCA; and the tyrosine-to-cysteine substitution at aa 570 (Y570C), which was identified in the most severe cases of CINCA associated with brain atrophy and episodes of epilepsy.[37] We first monitored cell death after transfection of the indicated CIAS1 mutants using annexin V as an indicator of phosphatidylserine exposure, and 7-AAD staining as an indicator of membrane damage. In THP-1 cells transfected with disease-associated mutants of CIAS1, the number of cells that were positive for both annexin V and 7-AAD dramatically increased as early as 3 hours after transfection. This profile of cell death was not observed in cells transfected with WT-*CIAS1* (Figure 1A), indicating that disease-associated mutations of *CIAS1* induced rapid cell death. Interestingly, the percentages of annexin V– or 7-AAD–positive cells were comparable with the level of ASC-dependent NF-κB activation by each of the disease-associated variants (Figure 1B).

When the expression of GFP-cryopyrin was monitored by flow cytometry, GFP began to become evident in cells at 1 hour and 30 minutes after transfection in both WT-*CIAS1*– and Y570C-transfected cells (Figure 1C). The expression of GFP-fusion protein was almost comparable between Y570C- and WT-transfected cells, up to 2 hours after transfection. At this point, the number of annexin V/7-AAD–positive cells increased only in Y570C-transfected THP-1 cells in a time-dependent manner (Figure 1C). Moreover, the percentage of annexin V– or 7-AAD–positive cells was almost comparable during the entire incubation period examined, suggesting that cells directly became annexin V/7-AAD–double-positive shortly after the initiation of gene expression. The efficiency of transfection was a approximately 75% in WT-*CIAS1*–transfected cells 3 hours after transfection, at which point 40% of Y570C-transfected cells were either annexin V or 7-AAD positive. At this point, the expression of GFP-fusion protein was reduced in Y570C-transfected cells (Figure 1C), most likely reflecting the decrease in cell viability.

To exclude the possibility that cell death induced by transfection of Y570C was due to the influence of the GFP moiety, WT-*CIAS1* and the disease-associated mutants of CIAS1 lacking the epitope tag were cloned into pIRES2-EGFP. Using this expression system, we confirmed that Y570C, but not WT-*CIAS1*, induced rapid cell death in THP-1 cells (Figure S1, available on the *Blood* website; see the Supplemental Materials link at the top of the online article). When we examined the another mammalian NLR NOD2/CARD15, and 2 of its disease-associated mutants, R334W and N670K, both of which are ligand-independent activating mutations observed in patients with Blau syndrome (MIM #186580) or early-onset sarcoidosis (MIM #609464),[36,38] neither WT nor disease-associated mutants of NOD2/CARD15 induced cell death (data not shown), indicating that the rapid cell death we observed was a specific phenomenon associated with CAPS-associated *CIAS1* mutations.

The cell death induced by Y570C is necrosis-like cell death

Disease-associated mutations in *CIAS1* induced rapid cell death, which exhibited features more similar to the necrosis seen in nigericin-treated cells rather than the apoptosis observed in actinomycin D–treated cells (Figure 1A). We were interested in evaluating other distinctive features of cell death, in addition to those observed using flow cytometry, that were induced by Y570C transfection. The amount of LDH released into the culture supernatant from Y570C-transfected cells was 28% at 2.5 hours and 45% at

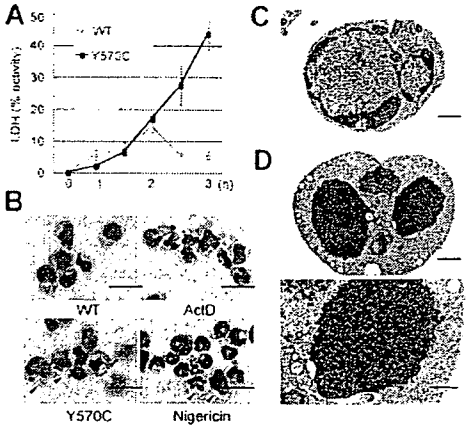

Figure 2. Distinctive features of cell death after Y570C transfection. (A) LDH release from damaged cells, as a percentage of total intracellular LDH content, which was set as 100%. The amount of LDH released into the culture supernatant from Y570C-transfected cells was significantly more than that released by WT-*CIAS1*–transfected cells. Error bars indicate SD (n = 3). (B) Cytospin preparations stained with Giemsa of the indicated cell populations and observed by inverted microscopy using an Olympus BX51 microscope (Olympus, Tokyo, Japan) equipped with a 40×/0.85 objective lens, an Olympus DP70 camera, and DP-controller version 1.1 software. Cells treated with 1 μg/mL actinomycin D (ActD) showed typical nuclear condensation with the formation of apoptotic bodies (white arrowheads), and slight cytoplasmic shrinkage. Some of the nuclei in nigericin-treated cells were swollen and stained weakly with Giemsa. In addition, nigericin-treated cells had larger cytoplasms, and were easily destroyed by the cytospin preparation process (black arrowheads). In Y570C-transfected cells, obvious nuclear condensation and formation of apoptotic bodies was rare, and their phenotypic appearance was similar to nigericin-treated necrotic cells. The scale bar represents 20 μm. (C) Electron microscopy of WT-*CIAS1*–transfected cells. The scale bar represents 1 μm. (D) Electron microscopy of Y570C-transfected cells revealed loss of the nuclear membrane cavity, and fusion of chromatin with the cytosol, as well as obscured structures of cytosolic organelles. The top scale bar represents 1 μm; the bottom scale bar represents 500 nm. Representative data from 3 independent analyses of similar results are shown.

3 hours after transduction, compared with total intracellular LDH content (which was set to 100%). This was significantly higher than that released by WT-transfected cells (8% at 2.5 hours and 3 hours), indicating that there was a rapid release of LDH from damaged cells (Figure 2A).

Cytospin preparations stained with Giemsa of WT-*CIAS1*– and Y570C-transfected cells are shown in Figure 2B. When cells were treated with actinomycin D, typical nuclear condensation and the formation of apoptotic bodies (white arrowheads in Figure 2B) was observed, along with slight shrinkage of the cytoplasm. In contrast, some of the nuclei in nigericin-treated cells were swollen, and were weakly positive for Giemsa staining. The cytoplasm in these cells was larger, and easily destroyed during cytospin preparation (black arrowheads in Figure 2B). In Y570C-transfected cells, obvious nuclear condensation and formation of apoptotic bodies was rare. Rather, the phenotypic appearance of these cells was similar to nigericin-treated necrotic cells (black arrowheads in Figure 2B). Examination of the cells using inverted microscopy showed that, after Y570C transfection, the cytoplasm of some cells became larger, with reduced reflection against visual light, and their nuclei more clearly identifiable, features which are associated with cellular edema (white arrowheads in Figure 3B). These features were also observed in nigericin-treated cells (data not shown). In addition, electron microscopy revealed the loss of the nuclear membrane cavity, and fusion of chromatin with the cytosol (Figure 2D), as well as obscured structures of cytosolic organelles, in agreement with the assessment of cellular edema based on inverted microscopy and the analysis of cytospin preparations. Thus, the features of rapid cell death induced by the CINCA-associated Y570C mutation were more like necrosis than apoptosis.

Necrosis, as the conceptual counterpart to apoptosis, occurs after exposure to high concentrations of detergents, oxidants, ionophores, or high intensities of pathologic insults, and is prevented only by removal of the stimuli. In contrast, programmed cell death is defined as a phenomenon that can blocked by an inhibitor of any signal pathway or activity (for example, caspases) within target cells.[27] Therefore, we examined the effect of a pancaspase inhibitor to inhibit cell death by disease-associated

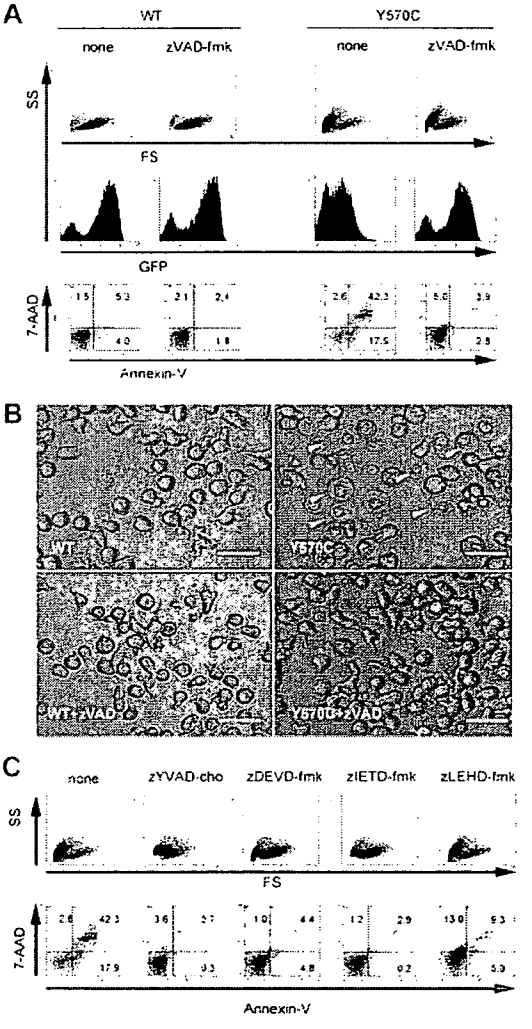

Figure 3. Suppressive effect of specific proteinase inhibitors on Y570C-induced cell death. (A) zVAD-fmk (50 μM) was added to THP-1 cells just after transfection. After transfection (3 hours), the cells were analyzed by flow cytometry. The expression of CIAS1 was monitored by GFP. Cells undergoing cell death appear as the cells smaller in size on the forward side-scatter (FS) axis, and cells positive for annexin V/7-AAD. The number in each quadrant shows the percentage of cells. (B) Transfected THP-1 cells were cultured in the presence or absence of 50 μM zVAD-fmk and observed by inverted microscopy using an Olympus IX70 microscope equipped with a 20×/0.40 objective lens and an Axiocam camera (Carl Zeiss). Axiovision version 3.0 software was used to process images. In some cells transfected with Y570C in the absence of zVAD-fmk treatment, the nucleus was more clearly delineated, and the cytoplasm was bigger in size but was less reflective of visual light (arrowheads), indicative of cells undergoing cell death. The scale bar represents 20 μm. (C) 50 μM of each caspase-specific inhibitor (caspase-1 inhibitor zYVAD-cho, caspase-3 inhibitor zDEVD-fmk, caspase-8 inhibitor zIETD-fmk, and caspase-9 inhibitor zLEHD-fmk) was added to THP-1 cells immediately after Y570C transfection, and cells were analyzed for cell death as for panel A. Representative data from 3 independent analyses of similar results are shown.

CIAS1 mutation. In the presence of 50 μM zVAD-fmk, the increase in cells that were double positive for annexin V and 7-AAD was suppressed (Figure 3A), even though the cell morphology profile represented by forward- and side-scatter window was not rescued by zVAD-fmk treatment. However, the inhibitory effect of the pancaspase inhibitor was also observed under inverted microscopy, in which the number of cells with a necrotic morphology after Y570C transfection was dramatically decreased by treatment with zVAD-fmk (Figure 3B).

Cell death induced by the disease-associated CIAS1 mutant is inhibited by a cathepsin B inhibitor

Because Y570C-induced cell death was inhibited by zVAD-fmk, we next examined the effect of specific inhibitors of each caspase. Caspase activation can occur via several routes, including the extrinsic pathway, characterized by death receptor–mediated recruitment and activation of apical caspase-8, and the intrinsic pathway, characterized by assembly of cytosolic Apaf-1 and mitochondrial cytochrome *c*, and subsequent activation of apical caspase-9.[39] Both of these pathways converge at the level of activation of executioner caspase-3.[40] Caspase-1, a member of the family of inflammatory caspases, is also known as IL-1β converting enzyme.[8] As shown in Figure 3C, the number of annexin V/7-AAD–double-positive cells observed after Y570C transfection in the absence of inhibitor (42.3%) unexpectedly decreased in the presence of each of the caspase inhibitors tested, including caspase-1 inhibitor zYVAD-cho (2.7%), caspase-3 inhibitor zDEVD-fmk (4.4%), caspase-8 inhibitor zITED-fmk (2.9%), and caspase-9 inhibitor zLEHD-fmk (9.3%). However, none of the caspase inhibitors rescued the cell morphology profile represented by the forward- and side-scatter window.

Although we could not identify the specific caspase-dependent cascade activated in Y570C-induced rapid cell death, it has been reported that zVAD-fmk and other caspase inhibitors are also potent cathepsin B inhibitors.[41] We next examined effect of the cathepsin B-specific inhibitor CA-074-Me on Y570C-induced cell death. CA-074-Me (50 μM) effectively inhibited ability of Y570C to induce cell death, as assessed by positive annexin V and 7-AAD staining (Figure 4A), and also rescued the cell morphology profile in the flow cytometry window representing forward and side scatter. Thus, disease-associated *CIAS1* mutation–induced cell death involves a cathepsin B–dependent pathway.

Disease-associated *CIAS1* mutation induces lysosomal leakage

Because cathepsin B is a lysosomal enzyme, we evaluated lysosomal functional integrity in Y570C-transfected cells by measuring the level of ssΔLL. Acridine orange preferentially accumulates in lysosomes, resulting in the appearance of red fluorescence after excitation with blue light,[42] whereas when this cationic dye is bound to DNA, it exhibits green fluorescence. In order to evaluate this green fluorescence, we used *CIAS1* and its variants without GFP in this study. When WT-*CIAS1*–transfected cells, as well as nontransfected cells, were incubated with acridine orange and examined by confocal laser microscopy, we observed a bright accumulation of red fluorescence in the lysosomes (Figure 4B). In these cells, we also observed fine structures in the nuclei that exhibited green fluorescence. In contrast, cytosolic red fluorescence was reduced in Y570C-transfected cells (white arrowheads in Figure 4B). In addition, green fluorescent structures in the nuclei became dim in cells that had also lost lysosome-associated red

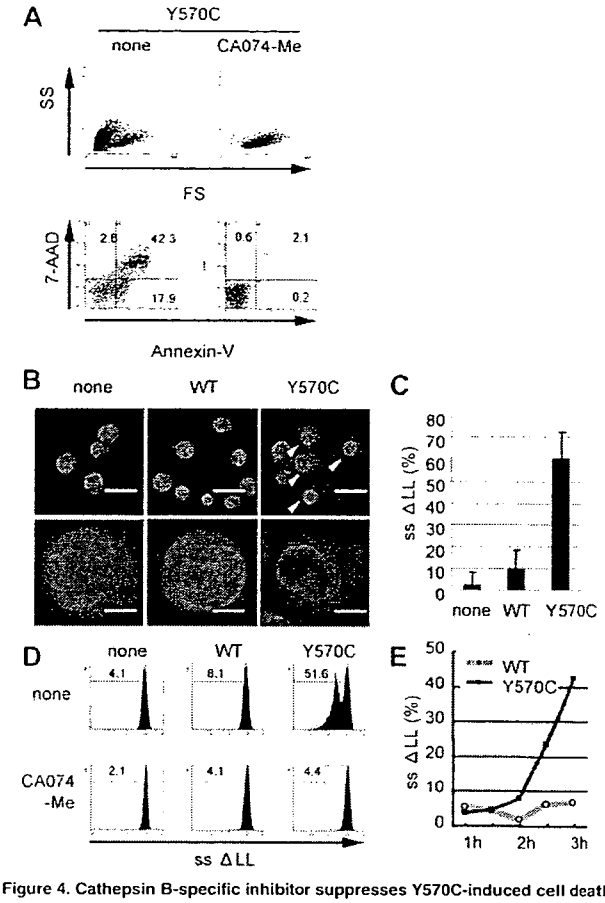

Figure 4. Cathepsin B-specific inhibitor suppresses Y570C-induced cell death and Y570C-transfection induces lysosomal leakage. (A) Y570C-transfected THP-1 cells were analyzed by flow cytometry 3 hours after transfection. Cells undergoing death are represented as cells that are smaller in size on the FS axis, and positive for annexin V/7-AAD. The cathepsin B–specific inhibitor CA-074-Me (50 μM) was added to THP-1 cells just after Y570C transfection. The number in each quadrant shows the percentage of cells. (B) Small-scale lysosomal leakage (ssΔLL) following transfection of WT-*CIAS1* and Y570C lacking the GFP epitope tag was assessed by incubating cells with 1 μg/mL of acridine orange and monitoring fluorescence using confocal laser microscopy. In Y570C-transfected cells, cytosolic red fluorescence was reduced, accompanied by a dimming of the green-fluorescent structures of the nuclei. The top scale bar represents 20 μm; the bottom represents 5 μm. (C) The percentage of the cells with ssΔLL 3 hours after transfection with either WT-*CIAS1* or Y570C. Error bars indicate SD (n = 6). (D) Analysis of ssΔLL by flow cytometry in cells transfected with the indicated constructs, in the presence or absence of 50 μM cathepsin B–specific inhibitor CA-074-Me. The cathepsin B–specific inhibitor CA-074-Me (50 μM) suppressed ssΔLL in Y570C-transfected cells. ssΔLL represents the loss of red fluorescence, and each number shows the percentage calculated in the region under the bar. (E) The percentage of cells with ssΔLL assessed by flow cytometry. Transfection with Y570C resulted in a time-dependent increase in ssΔLL in THP-1 cells. Representative data from 3 independent analyses of similar results are shown.

fluorescence. The percentage of the cells exhibiting ssΔLL after Y570C transfection (Figure 4C) was almost comparable with the percentage of cells that became annexin V/7-AAD positive in experiments performed side by side with GFP-tagged proteins (data not shown). Using flow cytometry, we found that the percentage of Y570C-transfected cells with ssΔLL increased in a time-dependent manner (Figure 4D), reaching 51.6% at 3 hours after transfection (Figure 4D). ssΔLL was also observed after transfection with other disease-associated mutations of *CIAS1* (Figure S2). This was also comparable to the results of annexin V/7-AAD staining. The induction of ssΔLL by Y570C transfection was effectively blocked with CA-074-Me (Figure 4D), suggesting

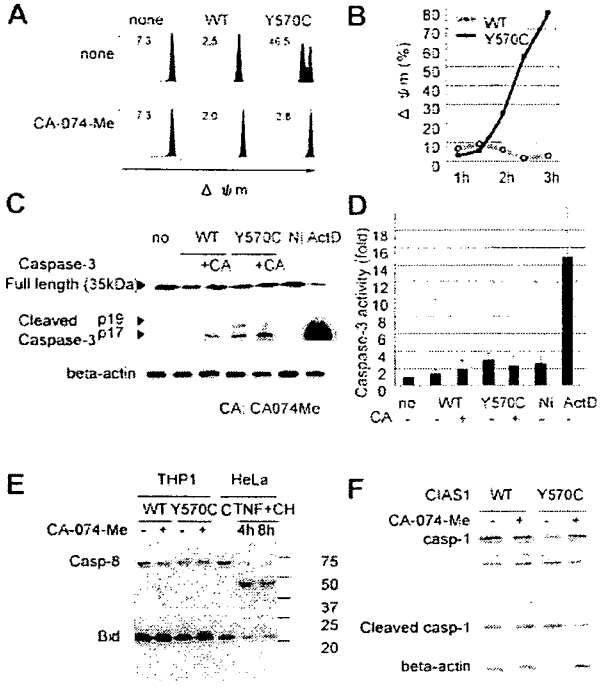

Figure 5. Y570C-transfection induces mitochondrial damage. (A) Loss of mitochondrial inner transmembrane potential (Δψm) was assessed by flow cytometry using 1 μM of MitoTracker DeepRed 633. Δψm is represented as the loss of deep red fluorescence. The cathepsin B–specific inhibitor CA-074-Me (50 μM) suppressed Δψm in Y570C-transfected cells. Each number shows the percentage calculated in the region under the bar. (B) The percentage of cells with Δψm increased in a time-dependent manner following transfection with Y570C. (C) Full-length caspase-3 was detected by using a caspase-3 antibody, and cleaved caspase-3 was detected by using a cleaved caspase-3–specific antibody. Y570C-tranfection resulted in slight cleavage of caspase-3. However, this level of cleavage was far less than that induced by actinomycin D (ActD) treatment, but similar to the level induced by nigericin treatment. (D) After transfection with the WT-*CIAS1* or Y570C mutant (3 hours), THP-1 cells were harvested and caspase-3 activity was measured according to the manufacturer's protocol. THP-1 cells treated with 1 μg/mL ActD and 20 μM nigericin (Ni) were used as controls. The fold increases in caspase-3 activity are the means of the normalized data (no treatment = 1) of triplicate cultures, and error bars indicate SD. (E) Neither cleaved caspase-8 nor Bid cleavage was observed upon Western blot analysis of cells following Y570C transfection. Bid cleavage can be assessed by the loss of full length of Bid. HeLa cells without treatment or treated with 20 ng/mL TNF-α and 10 μg/mL cycloheximide (TNF + CH) were used as positive controls for protein cleavage. (F) Y570C transfection did not induce caspase-1 cleavage at least 3 hours after transfection. Representative data from 3 independent analyses of similar results are shown.

that there may be paracrine/autocrine amplification pathway of cathepsin B–induced lysosomal leakage.

Disease-associated *CIAS1* mutation induces mitochondria damage

To further evaluate the mechanism of cell death induced by CAPS-associated *CIAS1* mutation, we assessed mitochondrial function using flow cytometry. Transfection with Y570C, but not WT-*CIAS1*, induced Δψm, indicating the presence of mitochondrial damage (Figure 5A-B). Interestingly, the percentage of cells with Δψm at 3 hours after transfection was most similar to GFP expression level, as represented in Figure 1C, and was greater than the number of cells that became annexin V/7-AAD positive, or showed ssΔLL after Y570C transfection (Figure 4E). Δψm was also observed after transfection with other disease-associated mutation of *CIAS1* (Figure S2). Treatment with CA-074-Me completely suppressed Δψm (Figure 5A), indicating that cathepsin B worked upstream from mitochondrial damage in CIAS1-induced cell death.

In some models of programmed cell death, it has been suggested that cathepsins act independently of caspases, whereas in other models, cathepsin-mediated cell death is caspase dependent.[26,27] In our experiments with each caspase-specific inhibitor, a specific caspase-dependent cascade was not evident. When Y570C was transfected into THP-1 cells, Western blotting showed that the cleavage of caspase-3 was slightly induced. However, cleavage was far less induced by Y570C transfection than by actinomycin D treatment (Figure 5C), even though there were no dramatic differences in the percentage of annexin V–positive cells (either PI-negative or -positive) between Y570C-transfected cells and actinomycin D–treated cells. Moreover, when caspase-3 enzyme activity was evaluated by using a colorimetric substrate, no increase in caspase-3 activity was observed after Y570C transfection (Figure 5D). On the other hand, when nigericin-treated THP-1 cells underwent necrosis, slight cleavage of caspase-3 was evident on the Western blots (Figure 5C), indicating that caspase-3 cleavage by disease-associated CIAS1 mutants may be accompanied by necrosis-like rapid cell death.

Apoptosis induced by forced oligomerization of ASC was reported to be mediated by caspase-8.[43] We observed no evidence of caspase-8 cleavage after Y570C transfection in our study (Figure 5E). Furthermore, it has been reported that caspase-1–dependent IL-1β activation is important in the necrosis-like cell death observed during *Salmonella* infection. However, Y570C transfection did not induce an apparent increase in caspase-1 cleavage (Figure 5F) within the time period of Y570C-induced rapid cell death.

Proapoptotic caspases are not likely to be directly activated by lysosomal proteases.[44-46] To identify the mechanism of lysosome-triggered cell death, we initiated a search for the cellular substrates of cathepsin B. One of the most likely cytosolic targets is Bid, a proapoptotic BH3-only Bcl-2 family member.[47,48] Bid has been reported to be a substrate of lysosomal proteases,[46] and in vitro studies indicate that lysosomal proteases can mediate cytochrome *c* release through Bid cleavage.[44] However, we did not observe Bid cleavage after Y570C transfection (Figure 5E), even though THP-1 cells contained high levels of full-length Bid.

R837, an activator of the cryopyrin-associated inflammasome, induces rapid cell death

Disease-associated mutations of *CIAS1* are thought to mimic active conformational changes in cryopyrin induced by microbial ligands. Recently, bacterial RNA and the small antiviral compound R837 were reported to activate caspase-1 through cryopyrin.[49] Addition of R837 to WT-*CIAS1*–transfected THP-1 cells induced rapid cell death, which was effectively suppressed by CA-074-Me (Figure 6A). R837-induced activation of NF-κB was confirmed using a reporter assay in HEK293 cells (Figure 6B). The basal level of NF-κB activity in mock-trasnsfected cells was set as 1. ASC-dependent NF-κB activation by WT-*CIAS1* (2.12 ± 0.02 fold; n = 3) increased approximately 2-fold with R837 treatment (5.12 ± 0.25 fold; n = 3). Interestingly, the ASC-dependent NF-κB activity of each of the disease-associated mutants also increased approximately 2-fold after R837 treatment (Figure 6B), even though R837 treatment did not increase the percentage of cells that were annexin V/7-AAD positive (Figure 6A).

On the other hand, addition of 2 μg/mL of MDP had only a marginal effect on cell death (Figure 6C). MDP also induced activation of NF-κB, but it did not show ASC dependency (Figure

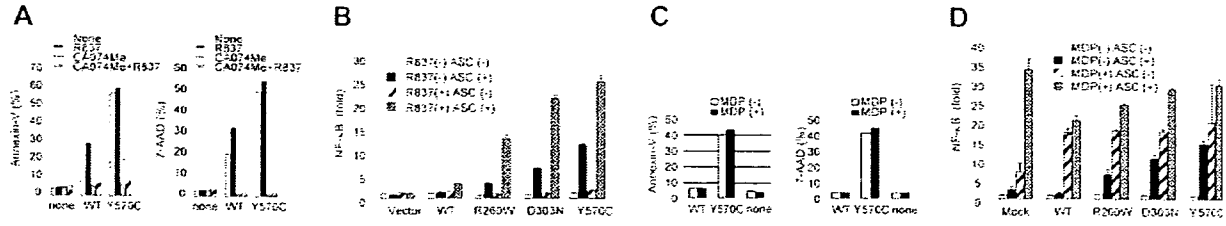

Figure 6. R837, activator of cryopyrin-associated inflammasome, induces rapid cell death. (A) Addition of 10 μg/mL imiquimod R837 to WT-*CIAS1*–transfected THP-1 cells induced rapid cell death, as assessed by annexin V– and 7-AAD–positive staining. This effect was effectively suppressed by CA-074-Me (CA074) treatment. (B) ASC-dependent-activation of NF-κB induced by R837 was assessed using a gene reporter assay in HEK293 cells in the presence or absence of 10 μg/mL R837. NF-κB activity in cells expressing each of the disease-related CIAS1 mutants increased approximately 2-fold after R837 treatment. Values represent the mean of normalized data (mock without R837 = 1) of triplicate cultures, and error bars indicate SD. (C) Addition of 2 μg/mL of MDP to WT-*CIAS1*– and Y570C-transfected THP-1 cells had only a marginal effect on cell death, as assessed by the percentage of cells that were positive for annexin V and 7-AAD. (D) ASC-dependent activation of NF-κB induced by MDP was assessed using a gene reporter assay in HEK293 cells in the presence or absence of 2 μg/mL MDP. Although MDP induced NF-κB activation, it did not show ASC dependency. Values represent the means of the normalized data (mock without MDP = 1) of triplicate cultures, and error bars indicate SD. Representative data from 3 independent analyses of similar results are shown.

6D). This is in contrast to a previous report that MDP induced IL-1β secretion from THP-1 cells as well as peripheral monocytes purified from a patient with CINCA.[50]

Discussion

More than 20 disease-associated mutations of *CIAS1* have been described in patients with FCAS, MWS, and CINCA, most of which are found within the centrally located NOD.[37,51,52] Of note, missense mutations similar to those found in *NOD2/CARD15* [51,53] have been identified in patients with Blau syndrome, another autosomal-dominant autoinflammatory syndrome, and early-onset sarcoidosis, a set of sporadic granulomatous disorders that are phenotypically similar to Blau syndrome. Amino acids affected by the R260W mutation in *CIAS1* and the R334W mutation in *NOD2/CARD15* are at analogous sequence positions, suggesting a common molecular mechanism for their role in the development of autoinflammatory disease. In addition to NF-κB activation and IL-1β production in PMA-treated THP-1 cells, in this study we showed that disease-associated mutations of *CIAS1* induced rapid cell death in THP-1 cells. Interestingly, CAPS-associated mutations in *CIAS1* induced a type of cell death that had several characteristic features of necrosis. Cells became annexin V/7-AAD double-positive shortly after the initiation of gene expression. Using inverted-microscopy and analysis of cytospin preparations, we demonstrated that Y570C-transfected cells had cellular edema without apparent nuclear condensation. These results were confirmed by electron microscopy. CAPS-associated mutations in *CIAS1* also provoked early LDH release, resulting in membrane damage. The protein encoded by *CIAS1*, cryopyrin, is homologous to plant disease resistance–associated NLRs, which mediate the hypersensitivity response, including metabolic alterations, production of antipathogen molecules, and localized cell death at the site of pathogen invasion.[54] Therefore, the rapid cell death induced within a few hours by activating CIAS1 may be a suitable response for protection against invading microorganisms. In addition, the cell death induced by *CIAS1* mutation was more characteristic of necrosis than typical apoptosis, and therefore may be more likely to evoke inflammation, a very reasonable response for "ringing the bell" in response to intruders.

Cell death induced by disease-associated *CIAS1* mutations was accompanied by lysosomal leakage, and loss of mitochondrial inner transmembrane potential. Interestingly, all of these effects were most significantly suppressed with the cathepsin B–specific inhibitor CA-074-Me. This indicates that disease-associated *CIAS1* mutation-induced cell death involves a cathepsin B–dependent pathway. Until recently, cathepsins were believed to be primarily involved in nonselective intracellular protein degradation in lysosomes, and their function outside lysosomes was largely discounted because of their instability at a neutral pH. However, cathepsins have transient activity in the cytosol, and as such, represent an enormous destructive potential. There are several examples of moderate lysosomal damage, often referred to as ssΔLL, leading to programmed cell death.[55,56] Unfortunately, the mechanism of cathepsin B release into the cytosol upon mutational activation of *CIAS1* remains unclear. It is possible that the method of gene transfection used in these studies induced lysosomal damage, and supported necrosis-like cell death of THP-1 monocytes. However, rapid cell death was not observed after the transfection with WT-*CIAS1* or Blau syndrome/early-onset sarcoidois-associated *NOD2/CARD15* under the same conditions, strongly suggesting that the cell death induced by CAPS-associated mutations in *CIAS1* was a specific phenomenon of the *CIAS1* mutants. On the other hand, our data indicated that cathepsin B participated in lysosomal leakage upon activation of CIAS1, since the induction of ssΔLL by disease-associated *CIAS1* mutations was effectively suppressed by CA-074-Me.

IL-1β reportedly plays an important role in the necrosis-like cell death observed during *Salmonella* infection. We found that the amount of IL-1β in cell-culture supernatants of PMA-treated THP-1 cells was very low, and almost comparable between Y570C- and WT-*CIAS1*–transfected cells at 4 hours after transfection (data not shown), a point at which rapid cell death had already been observed in Y570C-transfected cells. In addition, we could not confirm the activation of caspase-1 by Western blot after transfection of Y570C. Among patients with autoinflammatory disorders, the remarkable response of patients with MWS/CINCA to the recombinant human IL-1 receptor antagonist anakinra suggests that IL-1β has a fundamental role in the pathogenesis of inflammation associated with mutations in *CIAS1*.[57] However, we believe that the contribution of caspase-1 and IL-1β may be less potent in CIAS1-induced cell death.

The disease-associated mutations in *CIAS1* are thought to mimic active conformational changes induced by microbial ligands. Through intramolecular interactions of their LRRs, cryopyrin and NOD2/CARD15 are maintained in an inactive conformation. This conformation is relieved by ligand recognition through the LRRs. Bacterial RNA and the small antiviral compound R837, as well as the ATP and gout-associated uric acid crystals, were recently reported to activate caspase-1 through cryopyrin.[49,58,59] In the current study, we demonstrated that R837 induced rapid cell

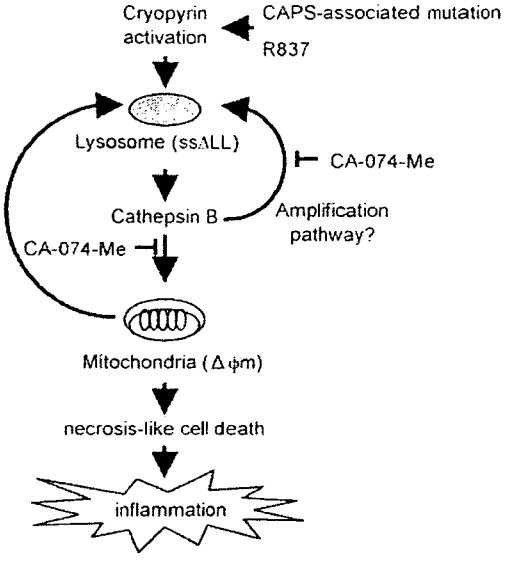

Figure 7. Activation of cryopyrin induces cathepsin B–dependent rapid cell death of human THP-1 monocytic cells. Activation of cryopyrin is induced by the CAPS-associated mutation or R837. It induces necrosis-like cell death, which is accompanied by lysosomal leakage (ssΔLL) and loss of mitochondrial inner transmembrane potential (Δψm). All of these effects are effectively suppressed by the cathepsin B–specific inhibitor CA-074-Me, indicating that the cell death involves a cathepsin B–dependent pathway. Unfortunately, the mechanism of cathepsin B release into the cytosol upon activation of CIAS1 remains unclear; however, there may be an amplification pathway that cathepsin B participated in further lysosomal leakage upon activation of CIAS1. Activation of cryopyrin induces cathepsin B–dependent rapid necrosis-like cell death, which has the potential to evoke inflammation.

death of WT-*CIAS1*–transfected THP-1 cells. R837 functions as a ligand for TLR7 and TLR8 in humans. Since THP-1 cells express endogenous TLR7, there remains a possibility that the rapid cell death observed after the incubation of cells with R837 was not only cryopyrin mediated, but also TLR7 mediated. However, as shown in Figure 6A, *CIAS1*-WT–transfected THP-1 cells were more sensitive to R837 than untransfected cells, suggesting that R837-induced cell death is mediated by cryopyrin. Although R837 is considered to be an activator of the cryopyrin-associated inflammasome, it is also possible that R837, like ATP, stimulates members of the P2X and P2Y family of purine receptors.[60]

Based on our results, we present the following model for cell death induced by activating mutations of *CIAS1* (Figure 7). The precise trigger for the release of cathepsin B remains unknown, but various insults, such as oxidative stress,[61,62] can destabilize the lysosomal membrane, thereby releasing lysosomal proteases into the cytosol. In fact, *CIAS1* was designated in association with FCAS, which is characterized by urticarial wheals, pain and swelling of joints, chills, and fever after exposure to cold stress. Following release of cathepsins into the cytosol, the initial response is magnified by the activation of cryopyrin, resulting in more lysosomal leakage. Released cathepsin B causes mitochondrial membrane dysfunction, but here as well, the mechanism remains to be fully elucidated, although it does not appear to involve Bid. Cytochrome *c* release from damaged mitochondria facilitates apoptosome formation, along with Apaf-1 activation and subsequent caspase-9, executioner caspase-3 and PARP activation. However, caspase-3 activation was not evident in our experiments, indicating that caspase-3 cleavage may be accompanied by necrosis-like rapid cell death. Cryopyrin-associated cell death may occur in a caspase-independent pathway.

In summary, cryopyrin, when activated, mediates rapid necrosis-like cell death in a lysosomal cathepsin B–dependent manner. Because cryopyrin is estimated to function as an intracellular pattern recognition receptor, cell death induced by putative activating mutations in *CIAS1* is more like necrosis-like cell death, which has the potential to evoke inflammation, a very reasonable response.

Acknowledgments

We thank Prof Nobuhiko Katunuma (Institute for Health Science, Tokushima Bunri University, Tokushima, Japan) for the fruitful discussion about lysosomal cathepsins, and Dr Yuji Horiguchi (Osaka Redcross Hospital, Osaka, Japan) for the electron microscopic observation.

This work was supported in part by grants-in-aid from the Ministry of Education, Science, Sports, and Culture, Japan.

Authorship

Contribution: A.F. performed the research and wrote the paper; N. Kambe and R.N. designed the research, analyzed the data, and helped in writing the paper; M.S. and H.T. performed and discussed the research; N. Kanazawa and S.A. analyzed and discussed the data; J.S. and T.S. contributed to plasmid constructions and provided helpful discussions; and T.H., T.N., and Y.M. managed and discussed the research.

Conflict-of-interest disclosure: The authors declare no competing financial interests.

Correspondence: Naotomo Kambe, Department of Dermatology, Kyoto University Graduate School of Medicine, 606-8507 Japan; e-mail: nkambe@kuhp.kyoto-u.ac.jp.

References

1. Yarom A, Rennebohm RM, Levinson JE. Infantile multisystem inflammatory disease: a specific syndrome? J Pediatr. 1985;106:390-396.
2. Prieur AM, Griscelli C, Lampert F, et al. A chronic, infantile, neurological, cutaneous and articular (CINCA) syndrome: a specific entity analysed in 30 patients. Scand J Rheumatol Suppl. 1987;66:57-68.
3. Aganna E, Martinon F, Hawkins PN, et al. Association of mutations in the NALP3/CIAS1/PYPAF1 gene with a broad phenotype including recurrent fever, cold sensitivity, sensorineural deafness, and AA amyloidosis. Arthritis Rheum. 2002;46:2445-2452.
4. Aksentijevich I, Nowak M, Mallah M, et al. De novo CIAS1 mutations, cytokine activation, and evidence for genetic heterogeneity in patients with neonatal-onset multisystem inflammatory disease (NOMID): a new member of the expanding family of pyrin-associated autoinflammatory diseases. Arthritis Rheum. 2002;46:3340-3348.
5. Dode C, Le Du N, Cuisset L, et al. New mutations of CIAS1 that are responsible for Muckle-Wells syndrome and familial cold urticaria: a novel mutation underlies both syndromes. Am J Hum Genet. 2002;70:1498-1506.
6. Feldmann J, Prieur AM, Quartier P, et al. Chronic infantile neurological cutaneous and articular syndrome is caused by mutations in CIAS1, a gene highly expressed in polymorphonuclear cells and chondrocytes. Am J Hum Genet. 2002;71:198-203.
7. Hoffman HM, Mueller JL, Broide DH, Wanderer AA, Kolodner RD. Mutation of a new gene encoding a putative pyrin-like protein causes familial cold autoinflammatory syndrome and Muckle-Wells syndrome. Nat Genet. 2001;29:301-305.
8. Martinon F, Tschopp J. Inflammatory caspases: linking an intracellular innate immune system to autoinflammatory diseases. Cell. 2004;117:561-574.
9. Ting JP, Davis BK. CATERPILLER: a novel gene family important in immunity, cell death, and diseases. Annu Rev Immunol. 2005;23:387-414.
10. Takeda K, Kaisho T, Akira S. Toll-like receptors. Annu Rev Immunol. 2003;21:335-376.
11. Inohara N, Chamaillard M, McDonald C, Nunez G. NOD-LRR proteins: role in host-microbial interactions and inflammatory disease. Annu Rev Biochem. 2005;74:355-383.
12. Inohara N, Nunez G. NODs: intracellular proteins

involved in inflammation and apoptosis. Nat Rev Immunol. 2003;3:371-382.

13. Inohara N, Ogura Y, Fontalba A, et al. Host recognition of bacterial muramyl dipeptide mediated through NOD2: implications for Crohn's disease. J Biol Chem. 2003;278:5509-5512.
14. Girardin SE, Boneca IG, Viala J, et al. Nod2 is a general sensor of peptidoglycan through muramyl dipeptide (MDP) detection. J Biol Chem. 2003; 278:8869-8872.
15. Chamaillard M, Hashimoto M, Horie Y, et al. An essential role for NOD1 in host recognition of bacterial peptidoglycan containing diaminopimelic acid. Nat Immunol. 2003;4:702-707.
16. Grenier JM, Wang L, Manji GA, et al. Functional screening of five PYPAF family members identifies PYPAF5 as a novel regulator of NF-kappaB and caspase-1. FEBS Lett. 2002;530:73-78.
17. Manji GA, Wang L, Geddes BJ, et al. PYPAF1, a PYRIN-containing Apaf1-like protein that assembles with ASC and regulates activation of NF-kappa B. J Biol Chem. 2002;277:11570-11575.
18. Srinivasula SM, Poyet JL, Razmara M, Datta P, Zhang Z, Alnemri ES. The PYRIN-CARD protein ASC is an activating adaptor for caspase-1. J Biol Chem. 2002;277:21119-21122.
19. Wang X, Kuivaniemi H, Bonavita G, et al. CARD15 mutations in familial granulomatosis syndromes: a study of the original Blau syndrome kindred and other families with large-vessel arteritis and cranial neuropathy. Arthritis Rheum. 2002;46:3041-3045.
20. Martinon F, Burns K, Tschopp J. The inflammasome: a molecular platform triggering activation of inflammatory caspases and processing of proIL-beta. Mol Cell. 2002;10:417-426.
21. Dowds TA, Masumoto J, Zhu L, Inohara N, Nunez G. Cryopyrin-induced interleukin 1beta secretion in monocytic cells: enhanced activity of disease-associated mutants and requirement for ASC. J Biol Chem. 2004;279:21924-21928.
22. Stehlik C, Reed JC. The PYRIN connection: novel players in innate immunity and inflammation. J Exp Med. 2004;200:551-558.
23. Agostini L, Martinon F, Burns K, McDermott MF, Hawkins PN, Tschopp J. NALP3 forms an IL-1beta-processing inflammasome with increased activity in Muckle-Wells autoinflammatory disorder. Immunity. 2004;20:319-325.
24. Masumoto J, Taniguchi S, Ayukawa K, et al. ASC, a novel 22-kDa protein, aggregates during apoptosis of human promyelocytic leukemia HL-60 cells. J Biol Chem. 1999;274:33835-33838.
25. Dowds TA, Masumoto J, Chen FF, Ogura Y, Inohara N, Nunez G. Regulation of cryopyrin/Pypaf1 signaling by pyrin, the familial Mediterranean fever gene product. Biochem Biophys Res Commun. 2003;302:575-580.
26. Guicciardi ME, Leist M, Gores GJ. Lysosomes in cell death. Oncogene. 2004;23:2881-2890.
27. Leist M, Jaattela M. Four deaths and a funeral: from caspases to alternative mechanisms. Nat Rev Mol Cell Biol. 2001;2:589-598.
28. Foghsgaard L, Wissing D, Mauch D, et al. Cathepsin B acts as a dominant execution protease in tumor cell apoptosis induced by tumor necrosis factor. J Cell Biol. 2001;153:999-1010.
29. Guicciardi ME, Miyoshi H, Bronk SF, Gores GJ. Cathepsin B knockout mice are resistant to tumor necrosis factor-alpha-mediated hepatocyte apoptosis and liver injury: implications for therapeutic applications. Am J Pathol. 2001;159:2045-2054.
30. Guicciardi ME, Deussing J, Miyoshi H, et al. Cathepsin B contributes to TNF-alpha-mediated hepatocyte apoptosis by promoting mitochondrial release of cytochrome c. J Clin Invest. 2000;106: 1127-1137.
31. Roberg K, Kagedal K, Ollinger K. Microinjection of cathepsin d induces caspase-dependent apoptosis in fibroblasts. Am J Pathol. 2002;161:89-96.
32. Roberg K, Ollinger K. Oxidative stress causes relocation of the lysosomal enzyme cathepsin D with ensuing apoptosis in neonatal rat cardiomyocytes. Am J Pathol. 1998;152:1151-1156.
33. Kagedal K, Zhao M, Svensson I, Brunk UT. Sphingosine-induced apoptosis is dependent on lysosomal proteases. Biochem J. 2001;359:335-343.
34. Hasegawa M, Imamura R, Kinoshita T, et al. ASC-mediated NF-kappaB activation leading to interleukin-8 production requires caspase-8 and is inhibited by CLARP. J Biol Chem. 2005;280: 15122-15130.
35. Saito M, Fujisawa A, Nishikomori R, et al. Somatic mosaicism of CIAS1 in a patient with chronic infantile neurologic, cutaneous, articular syndrome. Arthritis Rheum. 2005;52:3579-3585.
36. Kanazawa N, Okafuji I, Kambe N, et al. Early-onset sarcoidosis and CARD15 mutations with constitutive nuclear factor-kappaB activation: common genetic etiology with Blau syndrome. Blood. 2005;105:1195-1197.
37. Neven B, Callebaut I, Prieur AM, et al. Molecular basis of the spectral expression of CIAS1 mutations associated with phagocytic cell-mediated autoinflammatory disorders CINCA/NOMID, MWS, and FCU. Blood. 2004;103:2809-2815.
38. Kambe N, Nishikomori R, Kanazawa N. The cytosolic pattern-recognition receptor Nod2 and inflammatory granulomatous disorders. J Dermatol Sci. 2005;39:71-80.
39. Adrain C, Martin SJ. The mitochondrial apoptosome: a killer unleashed by the cytochrome seas. Trends Biochem Sci. 2001;26:390-397.
40. Hengartner MO. The biochemistry of apoptosis. Nature. 2000;407:770-776.
41. Schotte P, Declercq W, Van Huffel S, Vandenabeele P, Beyaert R. Non-specific effects of methyl ketone peptide inhibitors of caspases. FEBS Lett. 1999;442:117-121.
42. Erdal H, Berndtsson M, Castro J, Brunk U, Shoshan MC, Linder S. Induction of lysosomal membrane permeabilization by compounds that activate p53-independent apoptosis. Proc Natl Acad Sci U S A. 2005;102:192-197.
43. Masumoto J, Dowds TA, Schaner P, et al. ASC is an activating adaptor for NF-kappa B and caspase-8-dependent apoptosis. Biochem Biophys Res Commun. 2003;303:69-73.
44. Stoka V, Turk B, Schendel SL, et al. Lysosomal protease pathways to apoptosis: cleavage of bid, not pro-caspases, is the most likely route. J Biol Chem. 2001;276:3149-3157.
45. Schotte P, Van Criekinge W, Van de Craen M, et al. Cathepsin B–mediated activation of the proinflammatory caspase-11. Biochem Biophys Res Commun. 1998;251:379-387.
46. Reiners JJ Jr, Caruso JA, Mathieu P, Chelladurai B, Yin XM, Kessel D. Release of cytochrome c and activation of pro-caspase-9 following lysosomal photodamage involves Bid cleavage. Cell Death Differ. 2002;9:934-944.
47. Luo X, Budihardjo I, Zou H, Slaughter C, Wang X. Bid, a Bcl2 interacting protein, mediates cytochrome c release from mitochondria in response to activation of cell surface death receptors. Cell. 1998;94:481-490.
48. Li H, Zhu H, Xu CJ, Yuan J. Cleavage of BID by caspase 8 mediates the mitochondrial damage in the Fas pathway of apoptosis. Cell. 1998;94:491-501.
49. Kanneganti TD, Ozoren N, Body-Malapel M, et al. Bacterial RNA and small antiviral compounds activate caspase-1 through cryopyrin/Nalp3. Nature. 2006;440:233-236.
50. Martinon F, Agostini L, Meylan E, Tschopp J. Identification of bacterial muramyl dipeptide as activator of the NALP3/cryopyrin inflammasome. Curr Biol. 2004;14:1929-1934.
51. Albrecht M, Domingues FS, Schreiber S, Lengauer T. Structural localization of disease-associated sequence variations in the NACHT and LRR domains of PYPAF1 and NOD2. FEBS Lett. 2003;554:520-528.
52. Hull KM, Shoham N, Chae JJ, Aksentijevich I, Kastner DL. The expanding spectrum of systemic autoinflammatory disorders and their rheumatic manifestations. Curr Opin Rheumatol. 2003;15: 61-69.
53. Albrecht M, Lengauer T, Schreiber S. Disease-associated variants in PYPAF1 and NOD2 result in similar alterations of conserved sequence. Bioinformatics. 2003;19:2171-2175.
54. Dangl JL, Jones JD. Plant pathogens and integrated defence responses to infection. Nature. 2001;411:826-833.
55. Li W, Yuan X, Nordgren G, et al. Induction of cell death by the lysosomotropic detergent MSDH. FEBS Lett. 2000;470:35-39.
56. Hampton MB, Orrenius S. Dual regulation of caspase activity by hydrogen peroxide: implications for apoptosis. FEBS Lett. 1997;414:552-556.
57. Hawkins PN, Lachmann HJ, Aganna E, McDermott MF. Spectrum of clinical features in Muckle-Wells syndrome and response to anakinra. Arthritis Rheum. 2004;50:607-612.
58. Martinon F, Petrilli V, Mayor A, Tardivel A, Tschopp J. Gout-associated uric acid crystals activate the NALP3 inflammasome. Nature. 2006;440:237-241.
59. Mariathasan S, Weiss DS, Newton K, et al. Cryopyrin activates the inflammasome in response to toxins and ATP. Nature. 2006;440:228-232.
60. Lich JD, Arthur JC, Ting JP. Cryopyrin: in from the cold. Immunity. 2006;24:241-243.
61. Boya P, Andreau K, Poncet D, et al. Lysosomal membrane permeabilization induces cell death in a mitochondrion-dependent fashion. J Exp Med. 2003;197:1323-1334.
62. Antunes F, Cadenas E, Brunk UT. Apoptosis induced by exposure to a low steady-state concentration of H_2O_2 is a consequence of lysosomal rupture. Biochem J. 2001;356:549-555.

+ MOD

Available online at www.sciencedirect.com

ScienceDirect

Blood Cells, Molecules, and Diseases xx (2007) xxx–xxx

BLOOD CELLS, MOLECULES, & DISEASES

www.elsevier.com/locate/ybcmd

The first confirmed case with C3 deficiency caused by compound heterozygous mutations in the *C3* gene; a new aspect of pathogenesis for C3 deficiency

Miyuki Kida [a], Hirotaka Fujioka [b], Yoshiyuki Kosaka [c], Kouhei Hayashi [c], Yukio Sakiyama [d], Tadashi Ariga [a,*]

[a] *Department of Pediatrics, Hokkaido University Graduate School of Medicine, N-15, W-7, Kita-ku, Sapporo, Hokkaido, Japan*
[b] *Department of Plastic Surgery, Bibai Rousai Hospital, Hokkaido, Japan*
[c] *Department of Hematology and Oncology, Hyogo Prefectural Kobe Children's Hospital, Hyogo, Japan*
[d] *Department of Human Gene Therapy, Hokkaido University Graduate School of Medicine, Hokkaido, Japan*

Submitted 29 October 2007

(Communicated by R. I. Handin, M.D., 02 November 2007)

Abstract

The complement system is an ancient cascade system that has a major role in innate and adaptive immunity. Component C3 is central to the three complement pathways. Hereditary compliment 3 (C3) deficiency characterized by severe recurrent infections and immune complex disorders is extremely rare disease. Since 1972, inherited C3 deficiency has been described in many families representing a variety of national origins; however, only 8 families of these cases have been identified their genetic defects. Interestingly, all except one (incomplete analysis) were shown to harbor homozygous *C3* gene mutations. Previously we proposed a hypothesis, based on the unique process of C3 synthesis; C3 deficiency is not inherited as a simple autosomal recessive trait. Here, we report the first confirmed case with C3 deficiency caused by compound heterozygous mutations. They were a novel one base insertion (3176insT) in exon 24 which is predicted to result in a frameshift and a premature downstream stop codon (K1105X) in exon 26, and a nonsense mutation of C3303G (Y1081X) in exon 26 which was previously reported as homozygous mutations. This confirmed case suggests that our proposed hypothesis has prospects of a new aspect of pathogenesis for C3 deficiency.

Keywords: Component C3; C3 deficiency; Compound heterozygous mutations

Introduction

Complement protein C3 (OMIM+120700) is the major protein in the complement system in plasma. Cloning of the *C3* gene (19p13.3–13.2) revealed that the precursor molecule consists of 1663 amino acids encompassed by 41 exons and is located on chromosome 19. Inherited deficiency of C3 is an extremely rare disease; thus far, only 10 patients from eight families have had their molecular defects identified which led to their C3 deficiency ~~[1–7]~~. It is notable that almost all mutations, which vary among each family group, were homozygous ~~[1–4,6,7]~~. At present, only two cases (from one family) were suspected as being caused by compound heterozygous mutations after an incomplete analysis [5]. C3 is synthesized through a unique process; the mature C3 molecule results from a C3 precursor, which is cleaved into the α and β chains, and then the two chains are subsequently liked by disulfide bonds [9]. Previously, we reported the 10th case with C3 deficiency that was due to a novel homozygous mutation, and proposed a pathogenetic hypothesis, based on the unique process of C3 synthesis, that C3 deficiency is not inherited as a simple autosomal recessive trait [3]. Some compound heterozygous mutations, such as some combinations of missense mutations

* Corresponding author. Fax: +81 11 706 7898.
E-mail address: tada-ari@med.hokudai.ac.jp (T. Ariga).

1079-9796/$ - see front matter © 2007 Elsevier Inc. All rights reserved.
doi:10.1016/j.bcmd.2007.11.002